Hindawi
Journal of Spectroscopy
Volume 2023, Article ID 6599002, 8 pages
https://doi.org/10.1155/2023/6599002

Research Article

Microstructural Changes of Bone after Soft Tissue Removal: ATR-FTIR and XRD Spectroscopies

Mohammad A. Alebrahim,[1] **M-Ali H. Al-Akhras**,[2] **Ahmad S. Al-Hiyasat**,[3] **Ali S. Ba Rajjash**,[2] **M. S. Mousa**,[4] **and Abdulla Al Darayseh**[5]

[1]*Department of Allied Medical Sciences, Faculty of Applied Medical Sciences, Jordan University of Science and Technology, Ar-Ramtha, Jordan*
[2]*Bio-Medical Physics Laboratory, Department of Physics, Jordan University of Science and Technology, Ar-Ramtha, Jordan*
[3]*Department of Conservative Dentistry, Faculty of Dentistry, Jordan University of Science and Technology, Ar-Ramtha, Jordan*
[4]*Department of Physics, Mutah University, Al-Karak, Jordan*
[5]*Emirates College for Advanced Education, Abu Dhabi, UAE*

Correspondence should be addressed to Mohammad A. Alebrahim; maalebrahim@just.edu.jo

Received 15 November 2022; Revised 27 April 2023; Accepted 4 May 2023; Published 12 May 2023

Academic Editor: Wee Chew

The structural alterations that may arise in boiled and nonboiled bones are often overlooked despite their critical importance in the development of defleshing techniques across various scientific disciplines. To elucidate the microstructural characteristics of bones following the removal of soft tissue through conventional methods, attenuated total reflectance Fourier-transform infrared (ATR-FTIR) and X-ray diffraction (XRD) spectroscopies were employed. Our findings indicate that the boiled water method resulted in higher crystallinity, as evidenced by the FTIR data, whereas the XRD data revealed the opposite. This underscores the notion that a direct comparison between these two techniques is unfeasible as they measure distinct crystallinity parameters. In addition, the cold water maceration method caused a significant reduction in collagen crosslinking, as evidenced by the lower index observed.

1. Introduction

The study of bones using Fourier-transform infrared spectroscopy (FTIR) and X-ray diffraction (XRD) has emerged as a crucial and complementary approach in bone research, providing invaluable insights into bone composition, structure, and properties [1–3]. These techniques have been widely employed in various scientific fields, including biomedical research, paleontology, archaeology, and forensic science, to elucidate the importance of bones in health, evolution, cultural heritage, and forensic investigations [4–10].

FTIR is a powerful technique that enables the analysis of bone composition at the molecular level [11–14]. It measures the absorption and transmission of infrared radiation by bone samples, providing information about the functional groups, organic molecules, and mineral content present in bones. FTIR can identify the presence of collagen, which is the predominant organic component of bones, as well as other biomolecules, such as lipids, proteins, and carbohydrates [15, 16]. It can also provide insights into the chemical bonds, crystalline structure, and mineralization process of bones, making it a valuable tool for assessing bone quality, health, and disease [17].

On the other hand, XRD is a technique that analyzes the crystalline structure of bone samples. It measures the diffraction of X-rays by the crystal lattice of bone minerals, such as hydroxyapatite, which is the main inorganic component of bones [18–21]. XRD provides information about the crystallographic orientation, size, and arrangement of mineral crystals in bones, which is critical in understanding their mechanical strength, stiffness, and mineralization

patterns [22]. XRD is highly sensitive to changes in bone mineral crystallinity, which can reflect alterations in bone development, aging, and pathology [23, 24].

Despite their differences, FTIR and XRD are highly complementary in bone studies. FTIR provides information about the organic and mineral content of bones, while XRD focuses on the crystalline structure of bone minerals. Together, they provide a comprehensive understanding of bone composition and structure, enabling researchers to obtain a holistic view of bone properties. For example, FTIR can reveal changes in the collagen content and structure, while XRD can provide insights into alterations in mineral crystallinity. This combined approach allows for a more comprehensive analysis of bone health, disease, and evolution.

However, it is important to note that FTIR and XRD can sometimes yield opposing results in terms of bone crystallinity. FTIR measures the absorption and transmission of infrared radiation, which can be affected by various factors, including the organic components of bones, water content, and sample preparation [25, 26]. As a result, FTIR can provide an overestimation or underestimation of bone crystallinity, depending on the specific conditions of the analysis. On the other hand, XRD directly measures the diffraction of X-rays by the crystal lattice of bone minerals, which is not influenced by the organic components of bones or water content [18]. Therefore, XRD is considered a more accurate technique for assessing bone crystallinity.

To reconcile the differences in bone crystallinity results obtained from FTIR and XRD, researchers often use calibration techniques, such as the conversion of FTIR spectra to a quantitative crystallinity index (CI) based on XRD data [27]. This allows for more accurate comparison and interpretation of results obtained from both techniques. In addition, other techniques, such as Raman spectroscopy and solid-state nuclear magnetic resonance (NMR), can also be used in conjunction with FTIR and XRD to further validate and corroborate findings related to bone studies [27, 28].

Hence, the primary objective of this study is to comprehensively explore the critical role of FTIR XRD in advancing bone research and elucidate the complementarity of these techniques in the bone study. Furthermore, this study also aims to investigate potential disparities in bone crystallinity outcomes that may arise when utilizing FTIR and XRD methods to provide a more comprehensive understanding of bone mineralization processes. By conducting a detailed analysis of these techniques, their strengths, limitations, and synergistic effects in bone research, this study seeks to contribute to the advancement of knowledge in the field of bone science and provide valuable insights for future research endeavors.

2. Materials and Methods

2.1. Sample Preparation. A complete femur bone from a single camel was purchased from a local retailer located in Irbid, Jordan. The femur bone was sectioned into cylindrical shapes and underwent tissue removal using a scalpel. The cylindrical bone pieces were divided into two groups, each consisting of ten randomly selected samples, for comparison of the microstructure. The first group underwent treatment using the bacterial cold water maceration technique, wherein the samples were immersed in a closed container filled with distilled water at room temperature for one week, with the water being replaced every two days to prevent mold growth [29]. Following cleaning with distilled water, the bone samples were air-dried for 48 hours at room temperature.

The second group, comprising 10 samples, underwent treatment via the bacterial warm water maceration technique. The bone samples were placed in a closed container filled with distilled water, which was brought to a boil, and were subjected to this temperature for 3 hours [30]. Following this, the samples were left in the container for 24 hours, allowing them to cool to room temperature. The boiled bone samples were then washed with distilled water and air-dried for 48 hours at room temperature to ensure consistency across all samples. Subsequently, all samples from both groups underwent analysis using ATR-FTIR spectroscopy and X-ray diffraction.

2.2. ATR-FTIR Spectroscopy. An FTIR instrument (TENSOR II, platinum ATR, Bruker Optik GmbH) equipped with a mercury-cadmium-telluride detector (MCT) was employed to obtain spectral data. The spectral range between 400 and 4000 cm^{-1} was scanned, as it corresponds to organic and inorganic compounds in bone. Each sample spectrum was collected as an average of 24 scans at a resolution of 4 cm^{-1}. To identify peak positions in our proposed spectral data, we used OriginPro software (version 2020) and applied a modified Savitzky–Golay filter with a window size of 11 and a polynomial order of 2 to the raw data. This filter was used to overcome background, dark current noises, and baseline drift. The second derivative method was applied to locate peak maxima and minima, and we used a threshold of 0.1 and a prominence criterion of 0.05 to filter out false peaks.

To determine the number of peaks to fit, we first examined the expected spectral features of our samples, which included the amide I band and the phosphate region. We compared our spectra to relevant literature references and previous experimental data to identify potential peak positions and assignments. We also performed a statistical analysis using a Gaussian mixture model to estimate the number of underlying peaks in the data. Based on these analyses, we selected ten peaks to fit in the amide I region and eleven peaks in the phosphate region. The band position centers were chosen to capture the major spectral features of our samples and were consistent with previous studies of similar compounds. We note that our peak identification and fitting approach may be influenced by the specific software and parameters used and may be subject to some degree of uncertainty.

2.3. X-Ray Diffraction (XRD). The X-ray diffraction (XRD) patterns of macerated bone were obtained using a Shimadzu LabX, XRD-6000 X-ray diffractometer in the 2θ range of 10–70° (Bragg angle) with a step size of 0.02°/min and a scan speed of 3.0 deg./min. The XRD measurements were

performed using a 40 kV and 20 mA X-ray diffractometer that generated CuKα radiation with a wavelength (λ) of 1.5406°A. The raw data were analyzed using Origin software.

2.4. Statistical Analysis. The crystallinity of the bone was determined through the 1020/1030 cm^{-1} ratio and full width at half maximum (FWHM) at 604 cm^{-1}, while collagen crosslinking (1660/1690 cm^{-1}) was analyzed by infrared spectroscopy. XRD was used to measure crystallinity and crystal size at the 002 patterns. Statistical analysis was performed to compare the results obtained from cold water and boiled water bone maceration methods for each analysis, using a two-sample t-test.

3. Results

3.1. ATR-FTIR and XRD Spectra. The ATR-FTIR spectra and the band positions of the relevant spectral features are shown in Figure 1. IR spectra were carried out in the frequency range of 400 to 4000 cm^{-1} to establish potential differences between the two bone maceration methods used in this study. It is important to note that none of the treatments resulted in the disappearance or appearance of new IR bands. Only differences in IR band intensity were observed. There were strong bands at 558 and 604 cm^{-1}, which were attributed to $PO4^{3-}v4$. Another prominent band was at 1012 cm^{-1}, which was assigned to $HPO4^{2-}$. Vibrational bands corresponding to the amide group and $CO3^{2-}$ were also evident. In the bone, there are peaks related to amides and organic matrix (CH bands).

To deconvolute overlapping specific bands, the deconvolution analysis technique (DAT) is utilized using OriginPro software (version 2020), as demonstrated in Figure 2. The position of bands was determined through previously published and analyzed similar materials from the literature and by calculating second derivatives. Gaussian band shapes and linear baselines were employed as input parameters on normalized spectral data. The number of bands was taken as minimum as possible to reach a regression coefficient r^2 value near unity [32–36].

Figure 3 displays the XRD spectra of the macerated bone. The crystalline phases present in the samples were identified by XRD using standard JCPDS 9-0432 cards available in the system software. The XRD spectra of the bone samples exhibited several peaks with strong intensities at angles between $25 \leq 2\theta \leq 26$, which correspond to the crystal plane 002, and angles between $30 \leq 2\theta \leq 34$, which correspond to the crystal plane 211. However, the profiles exhibited similar peak positions with differences in peak intensity and width. In this study, we focused on the 002 pattern in our calculations to compare the crystallinity and calculate the crystal size of the bone samples after the maceration process.

3.2. IR Analysis of Crystallinity Index and Collagen Crosslinks in Bones. Bone crystallinity was determined using the traditional band intensity ratio of 1030/1020 cm^{-1} and the full width at half maximum (FWHM) of the peak at 604 cm^{-1}. The collagen crosslinking index was estimated by the intensity ratio of the subbands at 1660 and 1690 cm^{-1}. These parameters were statistically analyzed and compared between the two methods (cold water and hot boiled water bone maceration) using a two-sample *t*-test for each analysis. The mean values of the crystallinity and collagen crosslinking in the bone samples are presented in Table 1.

In the IR analysis, the mean values of the crystallinity based on the 1030/1020 cm^{-1} band intensity ratio for the boiled water group were slightly higher than those of the cold water group, although the difference was relatively small, it was statistically significant ($p = 0.008$), as determined by the *t*-test. The mineral crystallinity index calculated based on the FWHM of the peak at 604 cm^{-1} is inversely proportional to the bandwidth of the peak. This peak provides direct information on the crystallinity index of the sample and corresponds to the apatitic phosphate environment. The narrower the peak, the higher the crystallinity index. Our analysis revealed that the mean values of the crystallinity based on the FWHM of the 604 cm^{-1} peak and the collagen crosslinking were significantly lower in the boiled water group than in the cold water group ($p < 0.001$).

3.3. XRD Analysis of Crystallinity and Crystal Size. Crystallinity is directly related to the degree of perfection and size of crystals, which is reflected by the inverse width of the (002) (c-axis reflection) in the bone mineral powder X-ray diffraction pattern. The Debye–Scherrer approximation [37] is used to calculate the average crystal size (D) from XRD data. Bragg's constant ($k = 0.94$), the full width at half maximum of the peak in radians (β), the X-ray wavelength ($\lambda = 0.1540598$ nm for CuKα), and the 2θ diffraction angle of the 002 peak (θ) are the parameters involved in the calculation:

$$D = \frac{(K\lambda)}{\beta 2\theta}. \quad (1)$$

In the XRD analysis, as presented in Table 2, the mean value of the crystallinity at FWHM 002 was found to be higher in the boiled water group than in the cold water group, but the crystal size was found to be smaller in the boiled water group than in the cold water group. These differences were statistically significant ($p = 0.001$ and $p = 0.002$, respectively). The individual sample readings within each group were observed to be very close to each other, resulting in a relatively small standard deviation in each group of the study.

4. Discussion

In this study, we assessed the variations and disparities in the organic and inorganic bone structure concerning the defleshing process, which was based on boiled water and cold water maceration. Two different analytical techniques were employed. The FTIR results indicated a significant change in bone crystallinity between the two maceration methods that were utilized to eliminate the soft tissue from the bone. The intensity ratio of 1030/1020 cm^{-1} was found to be higher in the boiled bone, and simultaneously, the

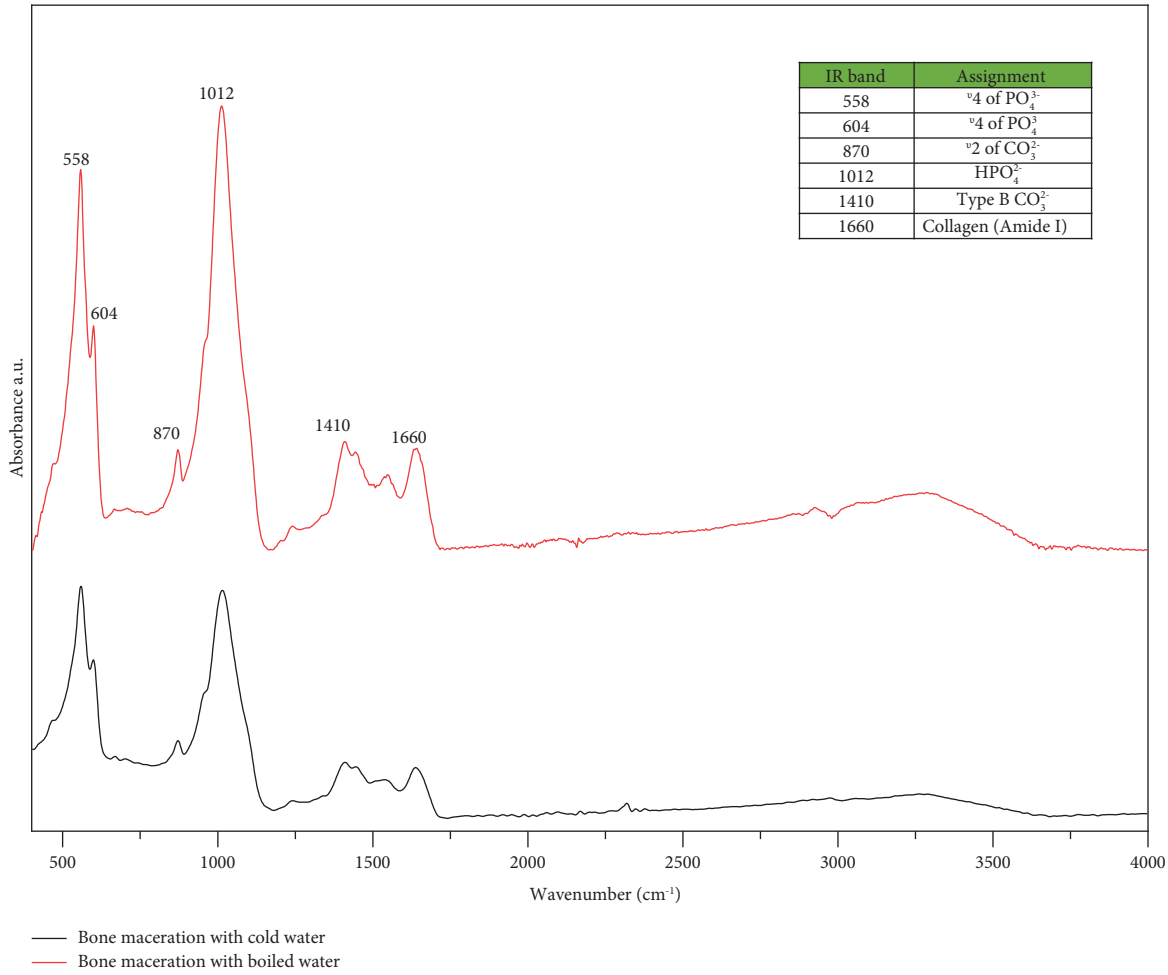

Figure 1: The ATR-FTIR spectra of bone maceration with boiled water (red) and bone maceration with cold water (black). The main infrared bands are assigned [31].

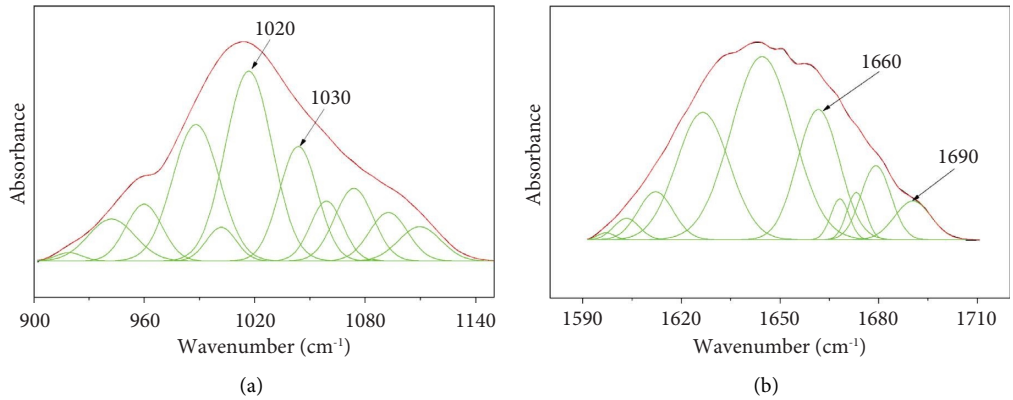

Figure 2: Curve-fitting analysis of the phosphate band (a) and amide I profile (b) of the IR bone spectra illustrated the subbands. The experimental spectrum (black) is overlaid with the reconstructed envelope (red), which is composed of fitted curves (green).

FWHM of the peak at 604 cm^{-1} was lower in the boiled bone. These findings suggest that the crystallinity of the boiled bone samples is greater than that of the bone samples that were treated with the cold water maceration method.

Previous research consistently demonstrates that hydroxyapatite changes to a purer form with larger crystals, higher crystallinity, and reduced porosity as the burning temperature increases [38], owing to the release of carbonate

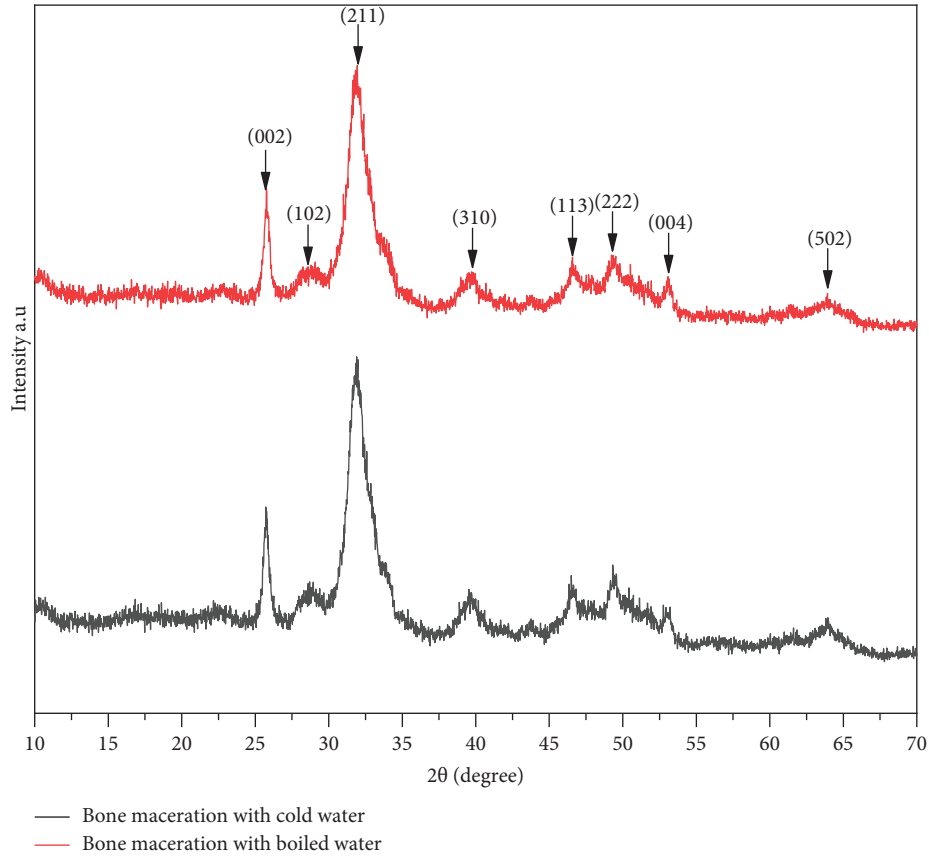

Figure 3: The XRD spectra of bone samples subjected to maceration with boiled water (red) and cold water (black).

Table 1: IR analysis of bone crystallinity and collagen crosslinking parameters (mean ± SD).

Maceration method	Crystallinity: 1030/1020 cm^{-1}	FWHM of 604 cm^{-1}	Collagen crosslinking
Cold water	0.977 ± 0.078	14.003 ± 0.848	2.404 ± 0.254
Boiled water	1.106 ± 0.086	11.062 ± 0.939	1.544 ± 0.298

Table 2: XRD analysis of bone crystallinity and its crystal size at 002 pattern (mean ± SD).

Maceration method	FWHM of 002 reflection	Crystal size at 002 reflection
Cold water	0.499 ± 0.042	17.178 ± 1.420
Boiled water	0.577 ± 0.022	14.767 ± 0.576

and water content [39]. In addition to the change in crystal size, there is also a significant alteration in the shape of the crystal, which occurs primarily between 500°C and 700°C [40, 41]. Although most studies on heated bone have focused on burned bone, only a few studies have been conducted on boiled bone. Consequently, there is a difference in the response of the bone when it is boiled as opposed to burning. Therefore, most studies on boiled bone have examined the change in the organic component of the bone, and there is evidence to suggest that there is a difference between the bone boiled in seawater and freshwater [42].

The findings suggest that the crystallinity of bone samples subjected to boiling was higher than those treated by the cold water maceration method, as per the results obtained through FTIR spectroscopy. It is important to note that these results are linked to the crystal bonds of the samples [27]. However, the XRD data revealed the opposite trend. The crystallinity index of the boiled bone samples was lower than that of the cold bone samples. These results are associated with the crystal structure arrangement of the samples [27]. In addition, the XRD data suggested a larger crystal size of bone samples in the cold water maceration method. Despite the increased use of crystallinity measures in bone structure studies, it remains uncertain whether these methods can be effectively applied without considering all the issues associated with their use and application. In other words, although various techniques can provide crystallinity parameters, the XRD values cannot be directly compared to those obtained from FTIR or Raman spectroscopy [43–45].

Crosslink chemistry is a crucial characteristic of type I collagen in the bone, providing it with high tensile strength and viscoelasticity through intermolecular crosslinking. FTIR has been employed to obtain insights into the protein structure through the underlying bands of the amid spectral

region. Of particular interest is the ratio of the sub-bands (1660/1690 cm^{-1}), which serves as a measure of the collagen crosslinks in the bone structure. The 1660 cm^{-1} band is associated with the presence of α-helix nonreducible (mature) collagen crosslinks, while the 1690 cm^{-1} band is linked to the reducible (immature) crosslinks.

Table 1 demonstrates that the collagen crosslinking index of macerated bone samples subjected to the boiled water method was lower than that of bone samples macerated in cold water. This indicates that temperature is a crucial factor in determining the organic bone profile. Specifically, the reduction in the crosslinking index is due to the decrease in the degree of molecular order of collagen [46]. Therefore, understanding the extent of collagen crosslinking in the bone is crucial in comprehending the overall impact of microstructural differences in the bone.

The findings of this study are limited due to several factors. Firstly, the use of specific animal remains as samples could affect the generalizability of the results. Although it has been previously suggested that a basic animal model of the bone can be employed to study the human bone due to the similarity in chemical composition between humans and mammals, there exist some differences in the microstructure of human and camel bones that could have an impact on the outcomes of this research. Secondly, while the study provides insight into the performance of two defleshing techniques and their effects on the bone tissue, conducting additional defleshing techniques could confirm the results. Lastly, further assessment of bone alteration techniques such as scanning electron microscopy (SEM) and Raman spectroscopy could be carried out to offer more comprehensive knowledge on the changes that could occur in the bone microstructure.

5. Conclusion

This study seeks to contribute to the understanding of the importance of using FTIR and XRD in bone research, their complementarity, and how potential discrepancies in bone crystallinity results can be reconciled. The findings of this study may have implications in various scientific fields, including biomedical research, paleontology, archaeology, and forensic science, enhancing our understanding of bone properties, health, disease, and evolution.

According to the FTIR data, bones treated with the boiled water method exhibited greater crystallinity, but the XRD data indicated the opposite. This suggests that a direct comparison between these two techniques is not feasible, as they measure different parameters of crystallinity. In addition, the collagen crosslinking was noticeably altered, with a reduced index observed in the cold water maceration method.

Data Availability

The data supporting the current study are available within this article.

Disclosure

A preprint has previously been published [47].

Conflicts of Interest

The authors declare that they have no conflicts of interest.

Authors' Contributions

Mohammad A. Alebrahim. conceptualized the study; Mohammad A. Alebrahim methodologized the study; Mohammad A. Alebrahim, Ahmad S. Al-Hiyasat, and Ali S B Rajjash provided the software.; formal analysis was performed by Mohammad A. Alebrahim and Ahmad S. Al-Hiyasat.; Mohammad A. Alebrahim wrote the original draft; Ahmad S. Al-Hiyasat reviewed and edited the manuscript, M-Ali H. Al-Akhras, Abdulla Al Darayseh, and M. S. Mousa reviewed and edited the manuscript.

Acknowledgments

The authors thank Jordan University of Science and Technology; Scientific Research's Deanship supported this research under Grant number: 594/2020.

References

[1] Ž. Mitić, A. Stolić, S. Stojanović et al., "Instrumental methods and techniques for structural and physicochemical characterization of biomaterials and bone tissue: a review," *Materials Science and Engineering: C*, vol. 79, pp. 930–949, 2017.

[2] P. L. Mahapatra, A. K. Singh, R. Tromer et al., "Energy harvesting using two-dimensional (2D) d-silicates from abundant natural minerals," *Journal of Materials Chemistry C*, vol. 11, no. 6, pp. 2098–2106, 2023.

[3] G. Paltanea, V. Manescu Paltanea, I. Antoniac et al., "A review of biomimetic and biodegradable magnetic scaffolds for bone tissue engineering and oncology," *International Journal of Molecular Sciences*, vol. 24, p. 4312, 2023.

[4] J. D. Fredericks, P. Bennett, A. Williams, and K. D. Rogers, "FTIR spectroscopy: a new diagnostic tool to aid DNA analysis from heated bone," *Forensic Science International: Genetics*, vol. 6, no. 3, pp. 375–380, 2012.

[5] C. Corti, S. Motella De Carlo, and L. Rampazzi, "The intimate soul of the pyres: new archaeological data from the terre di Rogo (pyre debris) of pre-roman necropolis in padua (northern Italy)," *Heritage*, vol. 6, pp. 849–866, 2023.

[6] S. Harikrishnan, S. D. George, S. Chidangil, and V. K. Unnikrishnnan, "Archaeophotonics: applications of laser spectroscopic techniques for the analysis of archaeological samples," *Applied Spectroscopy Reviews*, pp. 1–37, 2023.

[7] J. Olsen, J. Heinemeier, K. M. Hornstrup, P. Bennike, and H. Thrane, "Old wood'effect in radiocarbon dating of prehistoric cremated bones?" *Journal of Archaeological Science*, vol. 40, pp. 30–34, 2013.

[8] M. A. Goldberg, P. V. Protsenko, V. V. Smirnov et al., "The enhancement of hydroxyapatite thermal stability by Al doping," *Journal of Materials Research and Technology*, vol. 9, pp. 76–88, 2020.

[9] P. D. Giorgi, R. S. Giuseppe, S. Legrenzi, and F. Puglia, "Orthopedic application of collagen-hydroxyapatite bone substitutes: a clinical perspective," in *Innovative Bioceramics in Translational Medicine II: Surgical Applications*, pp. 247–263, Springer Singapore, Singapore, 2022.

[10] T. Nakano, Y. Umakoshi, and A. Tokumura, "Variation in crystallinity of hydroxyapatite and the related calcium

phosphates by mechanical grinding and subsequent heat treatment," *Metallurgical and Materials Transactions A*, vol. 33, no. 3, pp. 521–528, 2002.

[11] C. Rey, B. Collins, T. Goehl, I. R. Dickson, and M. J. Glimcher, "The carbonate environment in bone mineral: a resolution-enhanced fourier transform infrared spectroscopy study," *Calcified tissue international*, vol. 45, pp. 157–164, 1989.

[12] C. V. M. Rodrigues, P. Serricella, A. B. R. Linhares et al., "Characterization of a bovine collagen–hydroxyapatite composite scaffold for bone tissue engineering," *Biomaterials*, vol. 24, pp. 4987–4997, 2003.

[13] M. M. Figueiredo, J. A. F. Gamelas, and A. G. Martins, "Characterization of bone and bone-based graft materials using ftir spectroscopy," *Infrared spectroscopy-life and biomedical sciences*, pp. 315–338, 2012.

[14] B. Gieroba, A. Przekora, G. Kalisz et al., "Collagen maturity and mineralization in mesenchymal stem cells cultured on the hydroxyapatite-based bone scaffold analyzed by ATR-FTIR spectroscopic imaging," *Materials Science and Engineering: C*, vol. 119, Article ID 111634, 2021.

[15] M. J. Collins, C. M. Nielsen-Marsh, J. Hiller et al., "The survival of organic matter in bone: a review," *Archaeometry*, vol. 44, pp. 383–394, 2002.

[16] M. M. Mata-Miranda, M. Guerrero-Ruiz, J. R. Gonzalez-Fuentes et al., "Characterization of the biological fingerprint and identification of associated parameters in stress fractures by FTIR spectroscopy," *BioMed Research International*, vol. 2019, Article ID 1241452, 10 pages, 2019.

[17] E. P. Paschalis, R. Mendelsohn, and A. L. Boskey, "Infrared assessment of bone quality: a review," *Clinical Orthopaedics and Related Research*, vol. 469, no. 8, pp. 2170–2178, 2011.

[18] S. Tadano and B. Giri, "X-ray diffraction as a promising tool to characterize bone nanocomposites," *Science and Technology of Advanced Materials*, vol. 12, no. 6, 2012.

[19] C. Rey, C. Combes, C. Drouet, and M. J. Glimcher, "Bone mineral: update on chemical composition and structure," *Osteoporosis International*, vol. 20, no. 6, pp. 1013–1021, 2009.

[20] I. Atemni, R. Ouafi, K. Hjouji et al., "Extraction and characterization of natural hydroxyapatite derived from animal bones using the thermal treatment process," *Emergent Materials*, vol. 6, pp. 551–560, 2023.

[21] D. V. Abere, S. A. Ojo, G. M. Oyatogun, M. B. Paredes-Epinosa, M. C. D. Niluxsshun, and A. Hakami, "Mechanical and morphological characterization of nano-hydroxyapatite (nHA) for bone regeneration: a mini review," *Biomedical Engineering Advances*, vol. 4, Article ID 100056, 2022.

[22] P. Fratzl, H. S. Gupta, E. P. Paschalis, and P. Roschger, "Structure and mechanical quality of the collagen–mineral nano-composite in bone," *Journal of materials chemistry*, vol. 14, pp. 2115–2123, 2004.

[23] N. Matsushima and K. Hikichi, "Age changes in the crystallinity of bone mineral and in the disorder of its crystal," *Biochimica et Biophysica Acta (BBA) - General Subjects*, vol. 992, no. 2, pp. 155–159, 1989 Aug 18.

[24] L. C. Bonar, A. H. Roufosse, W. K. Sabine, M. D. Grynpas, and M. J. Glimcher, "X-ray diffraction studies of the crystallinity of bone mineral in newly synthesized and density fractionated bone," *Calcified Tissue International*, vol. 35, no. 1, pp. 202–209, 1983.

[25] M. M. Beasley, E. J. Bartelink, L. Taylor, and R. M. Miller, "Comparison of transmission FTIR, ATR, and DRIFT spectra: implications for assessment of bone bioapatite diagenesis," *Journal of Archaeological Science*, vol. 46, pp. 16–22, 2014.

[26] C. Gu, D. R. Katti, and K. S. Katti, "Photoacoustic FTIR spectroscopic study of undisturbed human cortical bone," *Spectrochimica Acta Part A: Molecular and Biomolecular Spectroscopy*, vol. 103, pp. 25–37, 2013.

[27] W. Querido, R. Ailavajhala, M. Padalkar, and N. Pleshko, "Validated approaches for quantification of bone mineral crystallinity using transmission fourier transform infrared (FT-IR), attenuated total reflection (ATR) FT-IR, and Raman spectroscopy," *Applied Spectroscopy*, vol. 72, no. 11, pp. 1581–1593, 2018.

[28] E. A. Taylor, C. J. Mileti, S. Ganesan, J. H. Kim, and E. Donnelly, "Measures of bone mineral carbonate content and mineral maturity/crystallinity for FT-IR and Raman spectroscopic imaging differentially relate to physical-chemical properties of carbonate-substituted hydroxyapatite," *Calcified Tissue International*, vol. 109, no. 1, pp. 77–91, 2021.

[29] G. Searfoss, *Skulls and Bones: A Guide to the Skeletal Structures and Behavior of North American Mammals*, Stackpole Books, Mechanicsburg, Pennsylvania, USA, 1995.

[30] S. J. Roberts, C. I. Smith, A. Millard, and M. J. Collins, "The taphonomy of cooked bone: characterizing boiling and its physico–chemical effects," *Archaeometry*, vol. 44, pp. 485–494, 2002.

[31] C. Lopes, P. H. J. O. Limirio, V. R. Novais, and P. Dechichi, "Fourier transform infrared spectroscopy (FTIR) application chemical characterization of enamel, dentin and bone," *Applied Spectroscopy Reviews*, vol. 53, pp. 747–769, 2018.

[32] E. I. Kamitsos, "Infrared studies of borate glasses," *Physics and Chemistry of Glasses*, vol. 2, pp. 79–87, 2003.

[33] A. M. Abdelghany, "The elusory role of low level doping transition metals in lead silicate glasses," *Silicon*, vol. 2, no. 3, pp. 179–184, 2010.

[34] A. M. Abdelghany, "Novel method for early investigation of bioactivity in different borate bio-glasses," *Spectrochimica Acta Part A: Molecular and Biomolecular Spectroscopy*, vol. 100, pp. 120–126, 2013.

[35] A. M. Abdelghany and A. Behairy, "Optical parameters, antibacterial characteristics and structure correlation of copper ions in cadmium borate glasses," *Journal of Materials Research and Technology*, vol. 9, pp. 10491–10497, 2020.

[36] M. A. Alebrahim, A. S. Al-Hiyasat, and A. S. B. Rajjash, "Effect of exposure to acidic food items on dentin characteristics: an ATR-FTIR study," *Advances In Materials Science And Engineering*, vol. 2022, Article ID 8542144, 7 pages, 2022.

[37] J. I. Langford and A. J. C. Wilson, "Scherrer after sixty years: a survey and some new results in the determination of crystallite size," *Journal of Applied Crystallography*, vol. 11, no. 2, pp. 102–113, 1978.

[38] M. J. D. F. M. D. Figueiredo, A. Fernando, G. Martins, J. Freitas, F. Judas, and H. Figueiredo, "Effect of the calcination temperature on the composition and microstructure of hydroxyapatite derived from human and animal bone," *Ceramics International*, vol. 36, pp. 2383–2393, 2010.

[39] X. Y. Wang, Y. Zuo, D. Huang, X. D. Hou, and Y. B. Li, "Comparative study on inorganic composition and crystallographic properties of cortical and cancellous bone," *Biomedical and Environmental Sciences*, vol. 23, no. 6, pp. 473–480, 2010.

[40] S. E. Etok, E. Valsami-Jones, T. J. Wess et al., "Structural and chemical changes of thermally treated bone apatite," *Journal of Materials Science*, vol. 42, no. 23, pp. 9807–9816, 2007.

[41] J. C. Hiller, T. Thompson, M. Evison, A. Chamberlain, and T. Wess, "Bone mineral change during experimental heating:

an X-ray scattering investigation," *Biomaterials*, vol. 24, pp. 5091–5097, 2003.

[42] A. Trujillo-Mederos, I. Alemán, M. Botella, and P. Bosch, "Changes in human bones boiled in seawater," *Journal of Archaeological Science*, vol. 39, pp. 1072–1079, 2012.

[43] S. Chakraborty, S. Bag, S. Pal, and A. K. Mukherjee, "Structural and microstructural characterization of bio-apatites and synthetic hydroxyapatite using X-ray powder diffraction and Fourier transform infrared techniques," *Journal of Applied Crystallography*, vol. 39, pp. 385–390, 2006.

[44] E. Pucéat, B. Reynard, and C. Lécuyer, "Can crystallinity be used to determine the degree of chemical alteration of biogenic apatites?" *Chemical Geology*, vol. 205, no. 1-2, pp. 83–97, 2004.

[45] E. T. Stathopoulou, V. Psycharis, G. D. Chryssikos, V. Gionis, and G. Theodorou, "Bone diagenesis: new data from infrared spectroscopy and X-ray diffraction," *Palaeogeography, Palaeoclimatology, Palaeoecology*, vol. 266, no. 3-4, pp. 168–174, 2008.

[46] M. Yousefi, F. Ariffin, and N. Huda, "An alternative source of type I collagen based on by-product with higher thermal stability," *Food Hydrocolloids*, vol. 63, pp. 372–382, 2017.

[47] M. A. Alebrahim, M. A. H. Al-Akhras, S. Ahmad et al., "Abdulla, microstructural changes of bone after soft tissue removal: ATR-FTIR and XRD Spectroscopies," 2023, https://ssrn.com/abstract=4064485.